Open charm production in DIS at HERA

S.Chekanov[a]

HEP Division, Argonne National Laboratory, 9700 S.Cass Avenue, Argonne,
IL 60439 USA

Presented at the International Europhysics Conference on High Energy Physics EPS (July 17th-23rd 2003) in Aachen, Germany

Abstract. An overview of recent HERA results on inclusive production of $D^{*\pm}$ mesons in deep inelastic scattering is given.

PACS. 12.38Bx Perturbative calculations – 12.38Qk Experimental tests

1 Introduction

The charm mass, m_c, is larger than the QCD dimensional scale Λ_{QCD}, therefore, perturbative QCD is applicable at the scale m_c. In deep inelastic scattering (DIS), another scale is the squared four-momentum transfer, Q^2, carried by the exchange photon. The conventional QCD interpretation for $Q^2 \sim m_c^2$ is that charm is determined solely by the gluon density, i.e. charm quarks are generated dynamically through the boson-gluon fusion (BGF) process. Such approach is called the fixed-flavour-number scheme (FFNS). For a sufficiently high Q^2, this description may not be adequate, thus the interplay between two independent scales, m_c and Q, embodies interesting QCD physics.

Since the charm quarks are copiously produced via gluon splitting, charm mesons can be used for testing different resummation techniques. The DGLAP resumption is often used together with the BGF process calculated up to next-to-leading-order (NLO) QCD (the HVQDIS program [1]). The BGF mechanism at leading-order QCD is implemented in parton-shower Monte Carlo (MC) models (AROMA [2] and RAPGAP [3]). Another description of the charm production is based on the CCFM evolution [4] as implemented in the CASCADE model [5]. This also starts from the BGF process but convoluted with the unintegrated gluon density.

The ZEUS analysis discussed in this overview was performed with the data (82 pb^{-1}) taken from 1998 to 2000, when electrons or positrons with energy $E_e = 27.6$ GeV were collided with protons of energy $E_p = 920$ GeV. The H1 Collaboration uses 1996-1997 data, when HERA operated with $E_p = 820$ GeV. In this paper, only high-statistics results based on reconstructed $D^{*\pm}$ mesons are discussed (other D mesons are discussed in [6]). The mesons were identified using the decay channel $D^{*+} \to D^0\pi^+$ with the subsequent decay $D^0 \to K^-\pi^+$ and corresponding antiparticle decay.

[a] For the H1 and ZEUS Collaborations

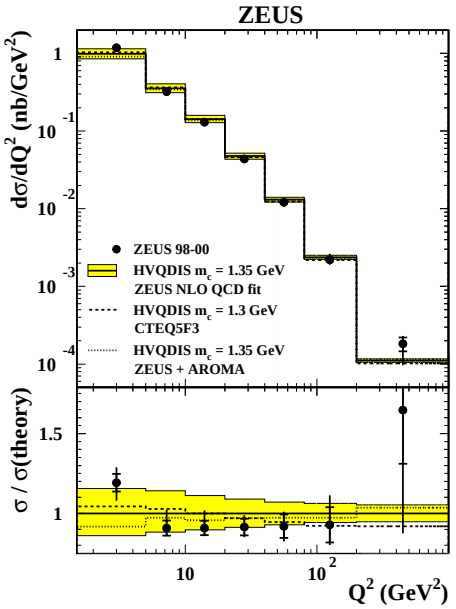

Fig. 1. Differential $D^{*\pm}$ cross section as a function of Q^2 for $0.02 < y < 0.7$, $1.5 < p_T(D^{*\pm}) < 15$ GeV and $|\eta(D^{*\pm})| < 1.5$, compared to the NLO QCD calculation of HVQDIS using the Peterson fragmentation with $\epsilon = 0.035$ and the hadronisation fraction $f(c \to D^*) = 0.235$ (solid line). The renormalisation and factorisation scales were set to $\sqrt{Q^2/4 + m_c^2}$. Also shown are the NLO QCD predictions based on the CTEQ5F3 PDF (dashed-dotted line) and an alternative hadronisation scheme (dotted line). The largest theoretical uncertainties (filled aria) are due to the charm mass (±0.15 GeV) and the scale variations ($0.5\mu_R$, $2\mu_R$).

2 Inclusive cross sections

Figure 1 shows the differential $D^{*\pm}$ cross section as a function of Q^2 [7]. The data falls by about four orders of magnitude in the measured region. The NLO QCD calcula-

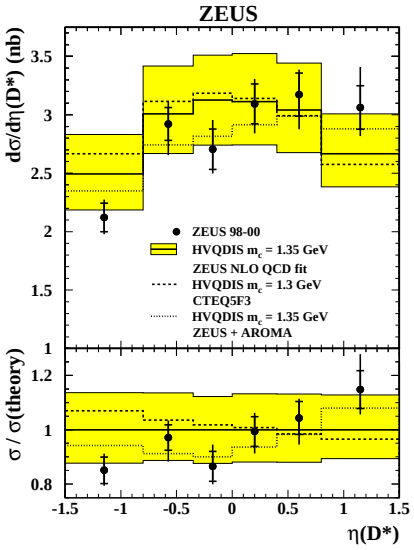

Fig. 2. Differential $D^{*\pm}$ cross sections as a function of $\eta(D^{*\pm})$ compared to the NLO QCD calculation of HVQDIS. The cross section was measured for $Q^2 > 1.5$ GeV^2. Other details as for Fig. 1.

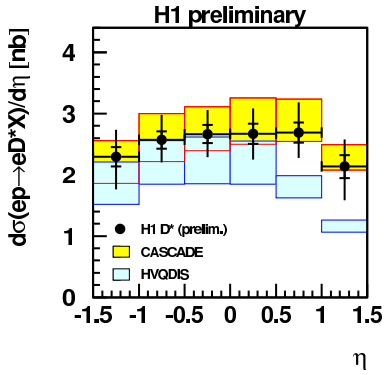

Fig. 3. Differential $D^{*\pm}$ cross section for $Q^2 > 2$ GeV^2 and $0.05 < y < 0.7$ as a function of $\eta(D^{*\pm})$ compared with the CASCADE and HVQDIS programs. The kinematic range for the $p_T(D^{*\pm})$ as for Fig.1. Both theoretical predictions are based on the Peterson fragmentation with the parameters as discussed in [10].

tions based on the FFNS give a good agreement with the measurements up to $Q^2 = 1000$ GeV^2. Predictions using an alternate PDF, CTEQ5F3, and the Lund-string hadronisation extracted from AROMA, instead of the Peterson fragmentation, are shown separately.

The pseudorapidity distribution of $D^{*\pm}$ mesons is known to be particularly sensitive to the underlying parton dynamics at small Bjorken x [8]. Figure 2 shows that the NLO calculation based on the ZEUS NLO fit [9], together with the Lund string fragmentation from AROMA, gives the best description of the $\eta(D^{*\pm})$ cross section (and also better than the prediction using GRV98-HO, not shown). The NLO predictions with the CTEQ5F3, and with the Peterson fragmentation, have distributions which are less shifted in the forward region.

The H1 Collaboration also observes differences between data and NLO QCD when the Peterson fragmentation and the CTEQ5F3 PDF is used for the NLO calculations [10], Fig. 3. The agreement with the data is better when the CASCADE model based on the CCFM evolution is used. Since both HVQDIS and CASCADE use the Peterson fragmentation, the difference between these models can be attributed to the parton dynamics at low x.

In contrast, ZEUS uses the MC models with the Lund string fragmentation. In Fig. 4, AROMA and CASCADE are compared with the data. The CASCADE overestimates the data, while AROMA is slightly below. The theoretical uncertainties, which are expected to be larger than for the NLO calculations, were not estimated. At present, data are not precise enough to distinguish between the shapes of the $\eta(D^{*\pm})$ distributions.

The resolved processes, in which the photon displays a hadronic structure, can contribute to the $D^{*\pm}$ cross section at low Q^2. The resolved contribution, as implemented in the RAPGAP model, enhances the $D^{*\pm}$ cross section in the rear direction [10]. Therefore, it is unlikely that the observed differences between the NLO QCD and the data can be explained by the resolved processes.

Generally, the description of the total charm cross section by MC models is not perfect. For more detailed tests, the total inclusive D^* cross section was calculated together with the D^* cross section with associated dijets [10], as shown in Fig. 5. The CASCADE model is systematically above the data, while RAPGAP (LO BGF) is below.

Figure 4 shows the ratio of e^-p and e^+p $D^{*\pm}$ cross sections as a function of $\eta(D^{*\pm})$ for $Q^2 > 1.5$ GeV^2. This ratio exhibits a trend to increase with increasing Q^2 and x [7]. For $Q^2 > 40$ GeV^2, there is $\sim 3\sigma$ difference between e^-p and e^+p $D^{*\pm}$ cross sections. According to the Standard Model, charm cross sections do not depend on the charge of the lepton in ep interactions. This difference is assumed to be a statistical fluctuation, and two sets of the data were combined. More e^-p data from HERA II is necessary to show whether the difference with the e^+p data is indeed a statistical fluctuation.

3 Extrapolation results

A popular way to look at double differential charm cross sections as functions of Q^2 and x is to reconstruct $F_2^{c\bar{c}}$. Integrated cross sections in Q^2 and y kinematic bins were extrapolated to the full phase space using HVQDIS based on the Peterson fragmentation function. Usually, several uncertainties in the extrapolation are considered. The largest uncertainties are those associated with the AROMA model for fragmentation and charm-mass variations (± 0.15 GeV).

Figure 6 shows the $F_2^{c\bar{c}}$as a function of x at Q^2 values between 2 and 500 GeV^2. The data rise with increasing Q^2; the rise becoming steeper at lower x. Comparisons of the ZEUS measurements [7] with previous results from H1 [11] show good agreement. The data are well described by the NLO prediction based on the ZEUS NLO QCD fit.

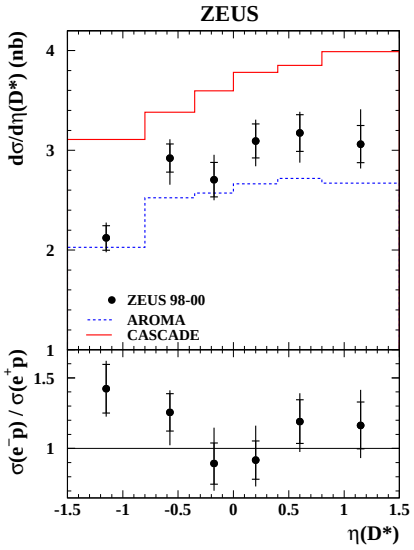

Fig. 4. Differential $D^{*\pm}$ cross section as a function of $\eta(D^*)$ compared with the AROMA (dashed line) and CASCADE (solid line) MC programs. Other details as for Fig.1.

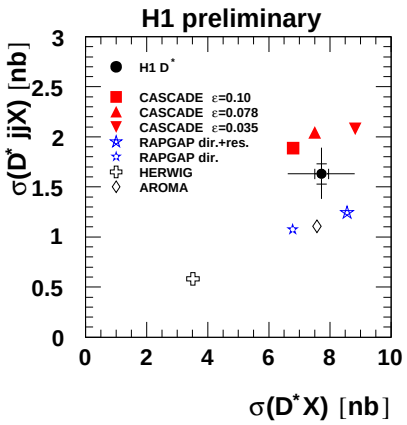

Fig. 5. The total inclusive $D^{*\pm}$ cross section versus the $D^{*\pm}$ cross section with associated dijet compared to MC models. The cross section was measured for $Q^2 > 2$ GeV^2, $0.05 < y < 0.7$ $1.5 < p_T(D^{*\pm}) < 15$ GeV and $|\eta(D^{*\pm})| < 1.5$. For the $D^{*\pm}$ cross section with associated dijets, $E_{T1} > 4$ GeV, $E_{T2} > 3$ GeV and $-1 < \eta(\text{jets}) < 2.5$ were applied.

4 Conclusions

The production of $D^{*\pm}$ mesons has been measured in DIS at HERA over a wide kinematic range in Q^2, from $Q^2 = 1.5$ GeV^2 to $Q^2 = 1000$ GeV^2. The NLO QCD based on the FFNS gives a good agreement with the data up to the highest Q^2 range measured.

At present, no conclusive statement can be made on the applicability of the CCFM evolution, since other effects related to charm fragmentation and the gluon density inside the proton, are shown to affect the $D^{*\pm}$ cross sections.

More data from HERA II is necessary to increase the precision of the measurements and to extend the kinematic range of reconstructed charm mesons. This should allow to understand the applicability of the FFNS at high Q^2 and the CCFM parton evolution at low x, as well as to understand whether there is a difference between e^-p and e^+p $D^{*\pm}$ data.

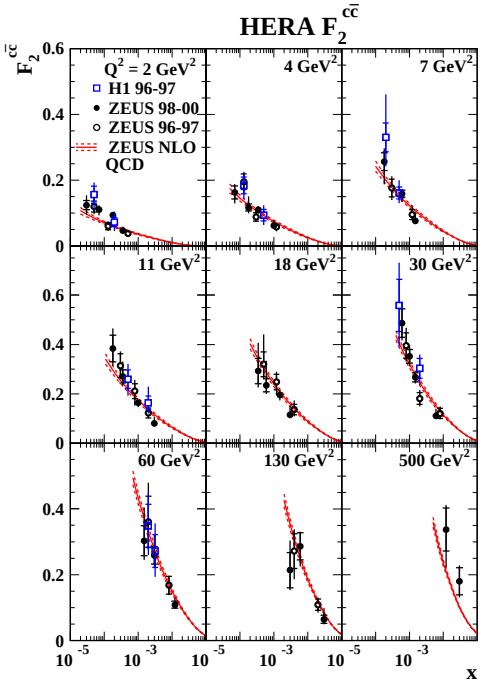

Fig. 6. The measured $F_2^{c\bar{c}}$ at Q^2 values between 2 and 500 GeV^2 as a function of x. The curves correspond to the result of the ZEUS NLO QCD fit, where the lower and upper curves show the uncertainty on the parton distributions for the ZEUS NLO fit.

References

1. B.W. Harris and J. Smith, Phys. Rev. **D 57**, (1998) 2806.
2. G. Ingelman and J. Rathsman, Comp. Phys. Comm. **101**, (1997) 135.
3. H. Jung, Comp. Phys. Comm. **86**, (1995) 147.
4. M. Ciafaloni, Nucl. Phys. **B 296** (1988) 49; S. Catani, F. Fiorani, G. Marchesini, Phys. Lett. **B 234** (1990) 339.
5. H. Jung, Comp. Phys. Comm. **143**, (2002) 100.
6. H1 Collaboration, paper submitted to this conference, *Measurement of Inclusive D-meson Production in DIS at HERA*, abstract 096.
7. ZEUS Collaboration, paper submitted to this conference, *Measurement of $D^{*\pm}$ production in deep inelastic $e^{\pm}p$ scattering at HERA*, abstract 563; see also ZEUS Collaboration, S. Chekanov et al., DESY 03-115 preprint, `hep-ex/0308068`.
8. S.P. Baranov et al., Eur. Phys. J. **C 24**, (2002) 425.
9. ZEUS Collaboration, S. Chekanov et al., Phys. Rev. **D 67**, (2003) 012007.
10. H1 Collaboration, paper submitted to this conference, *Inclusive D^* Meson and Associated Dijet Production in DIS*, abstract 074.
11. H1 Collaboration. C. Adloff et al., Phys. Lett. **B 528** (2002) 199.